Electronic Supplementary Information

Hydrophobic Dispersion-derived Si/rGO Nanocomposites in SiOC Ceramic Matrix as Anode Materials for High Performance Lithium-Ion Batteries

Minkyeong Ku[a], Dohyub Park[a], Minjun Kim[a], Minsu Choi[a], Wonchang Choi[a*]

[a]Department of Energy Engineering, Konkuk University, 120, Neungdong-ro, Gwangjin-gu, Seoul 05029, Republic of Korea

*Corresponding author Tel.: +82 2-2049-6051

E-mail address: wcchoi@konkuk.ac.kr (Prof. W. Choi)

Calculation for the composition (weight ratio) of each material in both composites based on TGA analysis results.

Assuming that the Si content is (x), the SiOC content is (1-x), and the rGO content is (y), the composition ratio of each material is calculated as follows.

[Si/SiOC composite]

$109.17x + 59.9(1 - x) = 68.5$

$49.27x = 8.6$

$x = 0.1745$

Si: 17.5 wt.% / SiOC: 82.5 wt.%

[Si/rGO/SiOC composite]

1) $109.17x + 59.9(1 - x) = 69.4$

$49.27x = 9.5$

$x = 0.1928$

2) $0.1928\ (x) : y = 94 : 6$

$y = 0.0123$

Si: 19.3 wt.% / rGO: 1.23 wt.% / SiOC: 79.47 wt.%

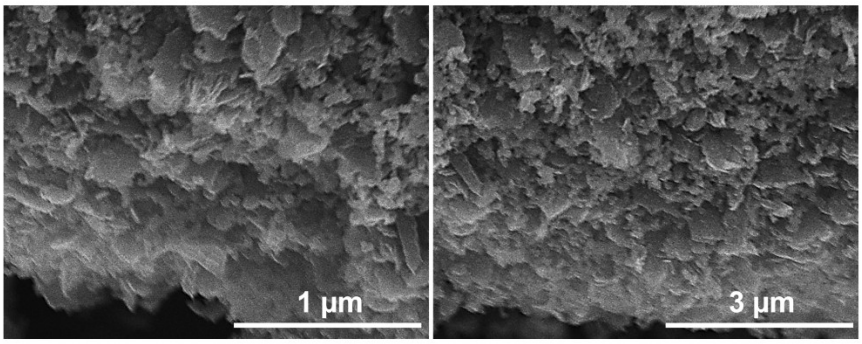

Fig. S1 FE-SEM images of TA-containing Si/rGO composite

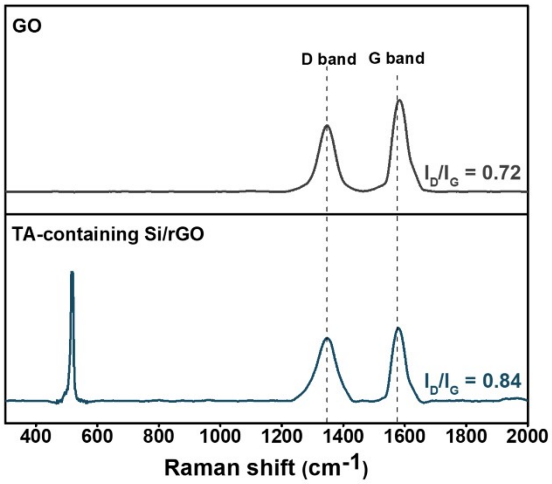

Fig. S2 Raman spectra of GO and TA-containing Si/rGO composite

In Fig. S2, TA-containing Si/rGO in this study exhibits an increased I_D/I_G, as compared to that of GO material. This result indicates that oxygen functional groups are removed to form atomic vacancies and decrease in sp^2 carbon domains, suggesting that GO was successfully reduced by TA.[1,2]

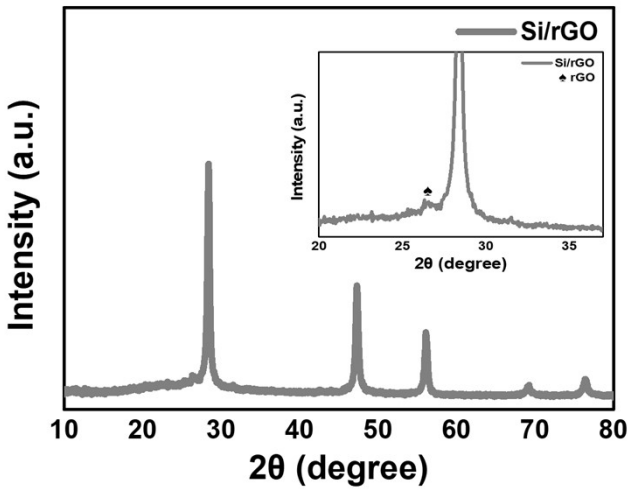

Fig. S3 XRD pattern of Si/rGO composite

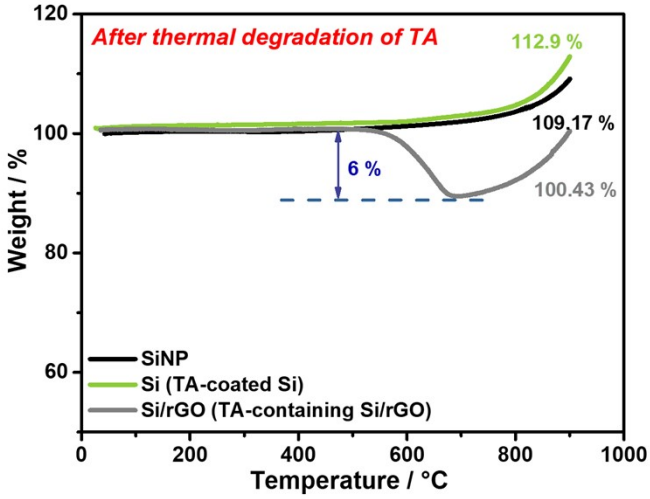

Fig. S4 TGA curves of SiNP, Si (TA-coated Si), and Si/rGO (TA-containing Si/rGO) after pyrolysis process in an inert gas atmosphere

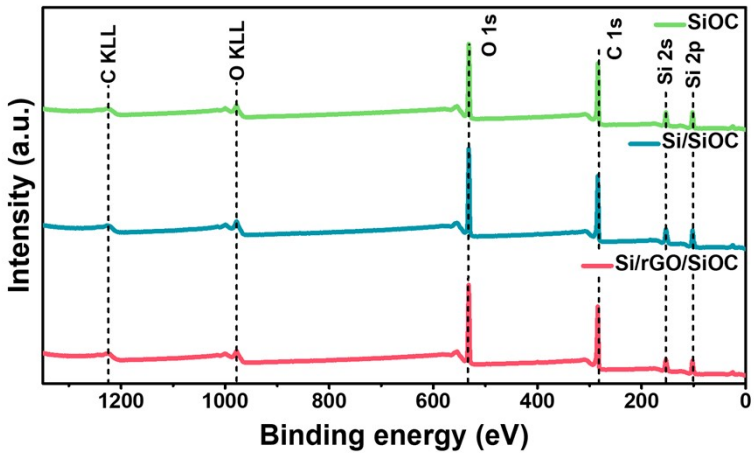

Fig. S5 XPS survey spectra of SiOC, Si/SiOC, and Si/rGO/SiOC composites

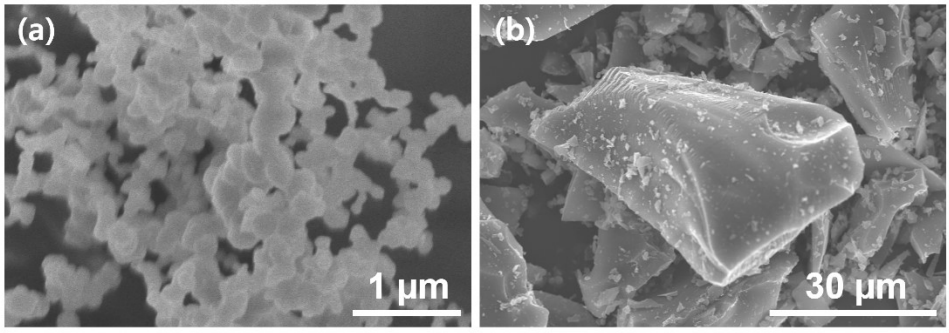

Fig. S6 FE-SEM images of: (a) SiNP and (b) SiOC

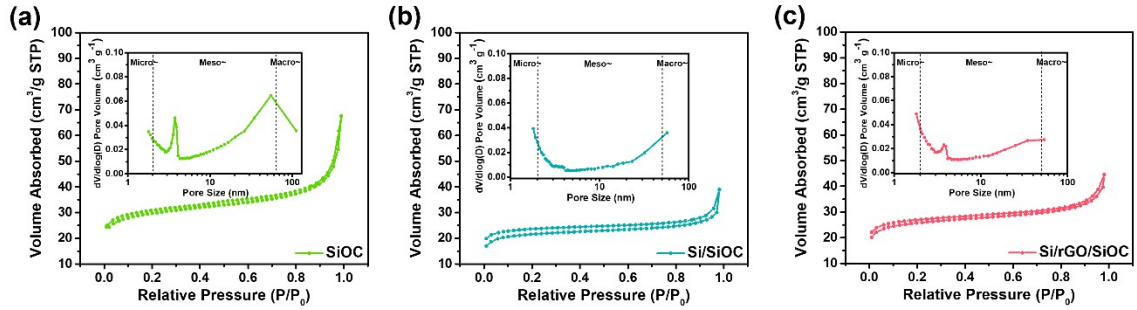

Fig. S7 Nitrogen absorption – desorption isotherm and corresponding pore size distribution (inset) of the (a) SiOC, (b) Si/SiOC, and (c) Si/rGO/SiOC

BET analysis was performed for SiOC, Si/SiOC, and Si/rGO/SiOC samples, and the measurement information is summarized in Table S1. All samples show mesoporous characteristics corresponding to a type IV isotherm curve. The Si/rGO/SiOC sample exhibits a relatively high surface area (92.82 m^2 g^{-1}) and pore volume (0.035 cm^3 g^{-1}), as compared to those of Si/SiOC, possibly owing to the large surface area of rGO.

Table S1. BET analysis results of the SiOC, Si/SiOC, and Si/rGO/SiOC

Sample	BET Surface Area (m^2 g^{-1})	Total pore volume (cm^3 g^{-1})	BJH Average pore size (nm)
SiOC	110.88	0.066	10.8
Si/SiOC	81.59	0.026	6.54
Si/rGO/SiOC	96.82	0.035	6.76

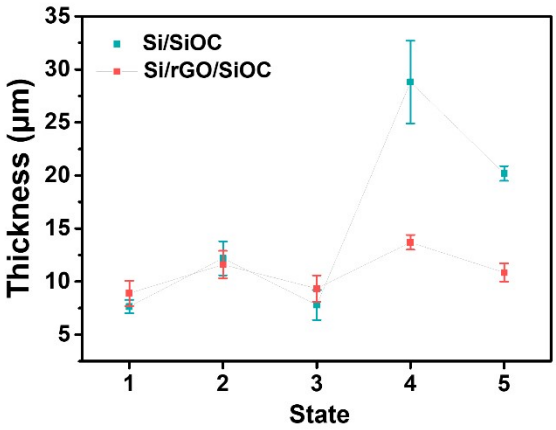

Fig. S8 Thickness of electrodes in each state of Si/SiOC and Si/rGO/SiOC electrodes

Table S2. Fitting values of Si/SiOC and Si/rGO/SiOC electrodes after 1 cycle and 100 cycles

	After 1 cycle			After 100 cycles		
	R_s (Ω)	R_{SEI} (Ω)	R_{ct} (Ω)	R_s (Ω)	R_{SEI} (Ω)	R_{ct} (Ω)
Si/SiOC	1.612	2.858	49.93	1.761	42.7	213.5
Si/rGO/SiOC	1.524	1.182	33.94	2.07	3.5	33.39

References

1. Y.-B. Kwon, S.-H. Go, C. Choi, T. H. Seo, B. Yang, M. W. Lee and Y.-K. Kim, *Diamond and Related Materials*, 2021, **119**.
2. Y. Lei, Z. Tang, R. Liao and B. Guo, *Green Chemistry*, 2011, **13**.